# Director dynamics in liquid-crystal physical gels

**Rafael Verduzco,[a] Neal R. Scruggs,[a] Samuel Sprunt,[b] Peter Palffy-Muhoray[c] and Julia A. Kornfield*[a]**

***Received 19th January 2007, Accepted 14th May 2007***
***First published as an Advance Article on the web 30th May 2007***
**DOI: 10.1039/b700871f**

Nematic liquid-crystal (LC) elastomers and gels have a rubbery polymer network coupled to the nematic director. While LC elastomers show a single, non-hydrodynamic relaxation mode, dynamic light-scattering studies of self-assembled liquid-crystal gels reveal orientational fluctuations that relax over a broad time scale. At short times, the relaxation dynamics exhibit hydrodynamic behavior. In contrast, the relaxation dynamics at long times are non-hydrodynamic, highly anisotropic, and increase in amplitude at small scattering angles. We argue that the slower dynamics arise from coupling between the director and the physically associated network, which prevents director orientational fluctuations from decaying completely at short times. At long enough times the network restructures, allowing the orientational fluctuations to fully decay. Director dynamics in the self-assembled gels are thus quite distinct from those observed in LC elastomers in two respects: they display soft orientational fluctuations at short times, and they exhibit at least two qualitatively distinct relaxation processes.

## Introduction

Depolarized dynamic light-scattering studies of nematic liquid crystals (LCs) give information about the dynamics of the nematic director (the axis of molecular orientational order). Small-molecule nematic LCs have two independent hydrodynamic modes, corresponding to splay-bend and twist-bend elastic distortions of director. These modes can be decoupled experimentally.[1] Addition of side-group liquid-crystal polymer (SGLCP) to a nematic solvent significantly slows these relaxation processes,[2] but qualitatively the relaxation dynamics are similar to those in small-molecule LCs. In the case of an LC elastomer or gel, network elasticity enters into the director dynamics.[3–5] LC elastomers are weakly cross-linked LC polymers, and LC gels are made by swelling elastomers in an LC solvent. In LC elastomers and gels, the director fluctuations are coupled to deformations of the network.

Here, we study LC physical gels formed by end-associating triblock copolymers.[6,7] Block copolymers are comprised of chemically distinct polymers covalently linked together. The present triblock copolymers consist of a side-group LC polymer (SGLCP) midblock flanked by polystyrene (PS) endblocks. When mixed with a small-molecule nematic LC, the PS–SGLCP–PS triblock copolymer forms aggregated structures, known as micelles, due to the different solubilities of the PS and SGLCP blocks. The PS blocks are relatively insoluble in the small-molecule LC, while the SGLCP block swells readily in the LC solvent. The triblock copolymers form an interconnected micellar network when mixed with an LC solvent. A key feature of these LC gels is that the physical cross-links can break and reform, and the network can reconfigure over time. The physical gels are therefore expected to behave like cross-linked elastomers on short time scales but give rise to behavior distinct from that of covalently cross-linked elastomers on long time scales.

The focus of this paper is on the orientational fluctuations in PS–SGLCP–PS physical gels and, for comparison, in homopolymer solutions of the SGLCPs on which the gels are based. The gels reveal overdamped fluctuations that relax over a broad time scale – ranging from "short" times ($<10^{-1}$ s and comparable to the director modes of the corresponding homopolymer solutions) out to much longer times ($\gg 10^{-1}$ s). The faster relaxation exhibits the $q^2$-dependence on scattering vector that is characteristic of hydrodynamic modes. We argue that the slow component of the fluctuations arises from the coupling of the nematic director to the physically associated polymers, which restructure on much longer time scales. The expression of this slow "gel" mode is anisotropic due to the orientational coupling between the polymer backbone and its pendant mesogenic groups, as in SGLCP homopolymers in nematic solvents.[2] The dynamics of physical LC gels, exhibiting a broadened spectrum combining *hydrodynamic* director modes and very slow relaxation associated with rearrangement of the gel structure, are thus quite distinct from previous studies of covalently bonded networks such as LC elastomers,[5] where light scattering reveals only director modes that are *non-hydrodynamic* due to a direct coupling of director rotation to network motion.

## Experimental

Polymer-analogous synthesis was used to make SGLCP homopolymers and coil–SGLCP–coil triblock copolymers with mesogens attached either "end-on" or "side-on" (Fig. 1). The end-on and side-on polymers preferentially orient with the backbone perpendicular or parallel, respectively, to the nematic director, resulting in an oblate (end-on) or prolate (side-on)

[a]*Division of Chemistry and Chemical Engineering, California Institute of Technology, 1200 East California Blvd., Pasadena, California, USA. E-mail: jak@cheme.caltech.edu*
[b]*Department of Physics, Liquid Crystal Institute, Kent State University, Kent, Ohio, USA. E-mail: sprunt@physics.kent.edu*
[c]*Liquid Crystal Institute, Kent State University, Kent, Ohio, USA. E-mail: mpalffy@lci.kent.edu*

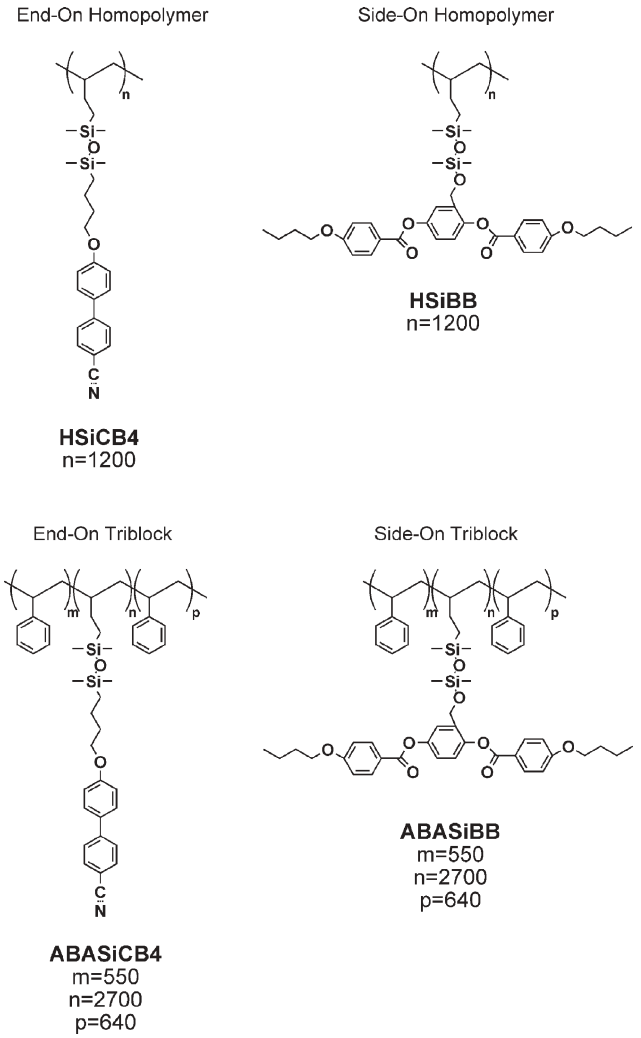


**Fig. 1** Chemical structure of the side-group LC homopolymers (HSiCB4 and HSiBB) and triblock copolymers (ABASiCB4 and ABASiBB).

chain conformation.[6] Mesogenic side-groups were attached to the pendant vinyl groups of an anionically polymerized 1,2-polybutadiene (PB) homopolymer (63 kg $mol^{-1}$) or a polystyrene-*b*-(1,2-polybutadiene)-*b*-polystyrene (57 kg $mol^{-1}$ PS, 140 kg $mol^{-1}$ PB, 67 kg $mol^{-1}$ PS) triblock copolymer according to published methods[7] (Fig. 1). The functionalized polymers contain a residual percentage of unmodified units in the form of unreacted 1,2-butadiene and non-reactive 1,4-butadiene present in the prepolymer (Table 1). All four polymers (Fig. 1) are nematic from room temperature up to a nematic–isotropic transition temperature ($T_{NI}$) (Table 1).

Solutions of these polymers in the nematic LC 4-pentyl-4′-cyanobiphenyl (5CB) were prepared by dissolving the polymer and 5CB together in dichloromethane (DCM), then evaporating the DCM under vacuum for at least one day. In this study, we focus most of our attention on 5 wt% polymer solutions.

Mixtures of polymer in 5CB were loaded into cells consisting of glass plates separated by 4, 9, or 25 μm spacers. Cells having 4 or 9 μm gaps were purchased from LC Vision (Boulder, CO, USA) and have $SiO_2$ alignment layers for homogeneous (planar) alignment. Cells having a 25 μm gap were purchased from EHC (Japan), and have rubbed polyimide alignment layers for homogeneous alignment. All three cell types have 5 × 5 mm transparent indium–tin oxide (ITO) electrodes in their centers. Cells were filled with polymer–LC solutions by capillary action; homopolymer solutions readily flowed in at room temperature and triblock gels flowed readily when heated above the gel point (35 °C for ABASiCB4, and 33 °C for ABASiBB). Homopolymer solutions spontaneously aligned to form monodomains under the influence of the alignment layers. Gels were made to form homogeneous monodomains by heating them above the gel point then slowly cooling them inside the bore of an 8 T NMR magnet with the field parallel to the alignment direction. Gels were also aligned to form homeotropic monodomains by heating them above the gel point then cooling while applying a 15 $V_{rms}$ potential difference across the ITO electrodes.

Aligned samples were mounted in a temperature-controlled oven with optical access that was stabilized to better than ±0.01 °C. The samples were illuminated with a focused, vertically polarized 20 mW HeNe laser beam (wavelength $\lambda_0$ = 633 nm) at normal incidence. Depolarized scattered light was collected at various scattering angles $\theta_s$, with the optical scattering vector $\boldsymbol{q}$ lying in the horizontal plane. Monodomain LC samples were placed in the beam oriented so that the nematic director was either parallel to the incident polarization (vertical, V), perpendicular to both the incident polarization and the incident beam (horizontal, H), or parallel to the incident beam (parallel, P) (Fig. 2). The time autocorrelation of the scattered intensity ($<I(q,0)I(q,t)>$ collected at discrete angles was recorded in the homodyne regime. The resulting intensity-autocorrelation functions were normalized by their maximum value, typically 1.95.

Each geometry probes primarily a particular elastic deformation.[2,8] The H and P geometries probe the twist-bend fluctuation mode of the LC director, with elastic-energy density $K_2 q_\perp{}^2 + K_3 q_z{}^2$, where $K_2$ and $K_3$ are twist and bend Frank elastic constants, respectively, and $q_z$ and $q_\perp$ are the components of $\boldsymbol{q}$ parallel and perpendicular to the director,

**Table 1** Polymer characteristics

| Polymer | Total $M_n$/kg $mol^{-1}$ | Polydispersity | LC Block $M_n$/kg $mol^{-1}$ | 1,2-PB content/mol % | 1,4-PB content/mol % | Mesogen content/mol % | $T_{NI}$/°C |
|---|---|---|---|---|---|---|---|
| H | 63 | 1.04 | N/A | 98 | 2 | N/A | N/A |
| HSiCB4 | 500 | 1.48 | 500 | 0 | 2 | 98 | 60 |
| HSiBB | 730 | 1.08 | 730 | 6 | 2 | 92 | 120 |
| ABA | 270 | 1.26 | N/A | 88 | 12 | N/A | N/A |
| ABASiCB4 | 1200 | 1.16 | 1100 | 0 | 12 | 88 | 40 |
| ABASiBB | 1400 | 1.5 | 1300 | 22 | 12 | 66 | 74 |

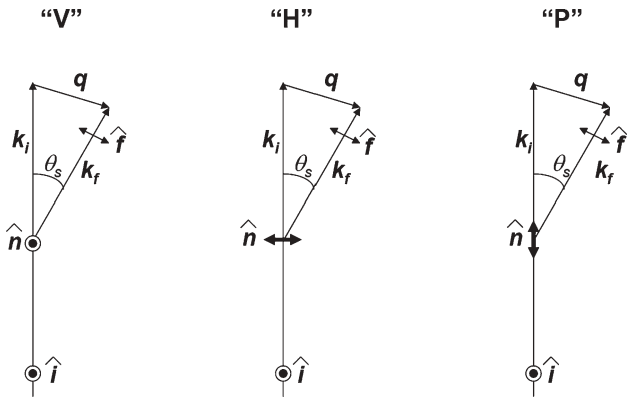


**Fig. 2** Top-view schematic of the three scattering geometries used. The scattering plane, which contains $\boldsymbol{q}$, is in the plane of the page, perpendicular to $\boldsymbol{i}$. Relative to the incident polarization, $\boldsymbol{i}$, and wavevector, $\boldsymbol{k_i}$, the LC director, $\boldsymbol{n}$, is oriented parallel to $\boldsymbol{i}$, ("V" for "vertical"), perpendicular to both $\boldsymbol{i}$ and $\boldsymbol{k_i}$ ("H" for "horizontal"), or parallel to $\boldsymbol{k_i}$ ("P" for "parallel"). The polarization direction of the analyzer, $\boldsymbol{f}$, is horizontal, perpendicular to $\boldsymbol{i}$. The intensity of the scattered, depolarized light is recorded at a discrete angle, $\theta_s$, in the laboratory frame, corresponding to a particular final wavevector, $\boldsymbol{k_f}$ and scattering vector $\boldsymbol{q} = \boldsymbol{k_f} - \boldsymbol{k_i}$.

respectively. In the H geometry, $q_z$ is dominant over most angles probed, and therefore the elastic energy is dominated by the bend contribution, except at small angles. In the P geometry, on the other hand, $q_\perp$ is the dominant contribution, and consequently the elastic energy is dominated by the twist distortions. Finally, in the V geometry, we detect both twist and splay fluctuations as separate modes, with energy densities $K_1 {q_\perp}^2$and $K_2 {q_\perp}^2$. The splay term is the dominant term, except at small angles.[2,8] Therefore, the dynamics observed in each geometry correspond to one of the three independent elastic deformations. Furthermore, $q^2$ scales as $\sin^2\theta_s/2$ in all the orientations, except at small $\theta_s$, where the effects of the LC birefringence may be significant.

The relaxation rates observed in dynamic light scattering are governed by the elastic-energy density that drives relaxation and the viscous dissipation associated with director reorientation. In small-molecule nematics and solutions of SGLCP in them, the resistance to reorientation is viscous and the relaxation times inherit the $q^2$-dependence of the elastic-energy density.[1,2] In elastomers and gels, additional viscous dissipation enters due to the network.[3–5]

As is common for liquid-crystal polymer light-scattering studies,[8,9] correlation functions from homopolymer solutions were fitted to the empirical Williams–Watts function,[10,11] $\exp(-t\Gamma)^\beta$ where $\Gamma$ is the relaxation rate and $0 < \beta < 1$ is a stretching exponent equal to one for purely exponential relaxation. If $\beta$ is assumed to result from a spectrum of relaxation times, the average relaxation rate $<\Gamma>$ may be calculated[12] from $\beta\Gamma/[\Gamma_1(\beta^{-1})]$, where $\Gamma_1$ denotes the Gamma function.

Prior to initiating a time-correlation experiment, the sample position was adjusted to a well-aligned region of the sample that minimized the static intensity of the scattered light. Monodomains of homopolymer solutions were highly uniform and required little adjustment. On the other hand, it was more difficult to achieve high-quality monodomains with gels, and more sample adjustment was required prior to each experiment.

On small (<100 nm) length scales, the gels have a heterogeneous structure that consists of an LC midblock solvated by the small-molecule LC and phase-separated endblocks swollen with LC. Over the length scales probed by our scattering experiment, ranging between approximately 350 nm and 2900 nm, the system can be considered homogeneous.

In some samples, and particularly for lower values of $\theta_s$, the intensity-autocorrelation function did not decay completely, even after several hours. For a few representative cases, we separately recorded correlation functions over several weeks, fully confirming that the data decay to a stable baseline and that the observed fluctuations are ergodic (or characteristic of a system in thermodynamic equilibrium), though very slow, due to the cross-linked polymer structure within the gel.

Previous rheological studies[7] confirm the existence of a broad plateau modulus in the physical gels. These results suggest that the physically associated block copolymers give rise to a gel with solid-like characteristics, and it follows from symmetry considerations that rotations of the nematic director are coupled to elastic distortions of the micellar network.[13,14] Furthermore, rheological studies of dilute (<3 wt%) gels reveal fluid-like behavior at low (<0.001 rad $s^{-1}$) frequencies. The plateau region of the 5 wt% gels extends to the lowest frequencies probed; hence, elastic character can be expected in the director-network coupling up to time scales of $10^4$ s or more. A transition to fluid-like behavior is expected at much longer times.

## Results

The comparison of intensity-correlation functions for 5CB, homopolymer solutions, and triblock gels presented in Fig. 3 reveals qualitatively different director-relaxation dynamics for each type of sample. In each orientation, 5CB shows single exponentially decaying relaxation modes, as has been previously established for small-molecule LCs.[1,15–17] Homopolymer solutions (with side-on and end-on SGLCPs, HSiBB and HSiCB4, respectively) exhibit stretched exponential time-correlation functions with significantly slower relaxation rates than for the small-molecule LC host, 5CB, in accord with prior literature on SGLCPs in nematic solvents.[2,9,18–21] The relaxation rates have the $q^2$-dependence associated with hydrodynamic modes (Fig. 4), as expected,[1,15–17] and the stretching exponent $\beta$ falls in the range of 0.57 to 0.99.

Addition of homopolymer with mildly oblate chain anisotropy (HSiCB4) slows relaxation more strongly in the H geometry than in the V geometry (Fig. 4b). The asymmetry is reversed for the polymer with strongly prolate chain anisotropy (HSiBB), which instead more strongly delayed relaxation in the V geometry (Fig. 4a). These results are in accord with extensive electro-rheological and light-scattering measurements by Jamieson and co-workers[2,9,18–21] and with a theoretical model by Brochard,[22] which predicts a strong reduction in director-bend relaxation rate (probed in the H geometry) relative to splay (probed in the V geometry) for the oblate homopolymer (with end-on mesogen attachment) and the opposite for the prolate homopolymer (side-on attachment).

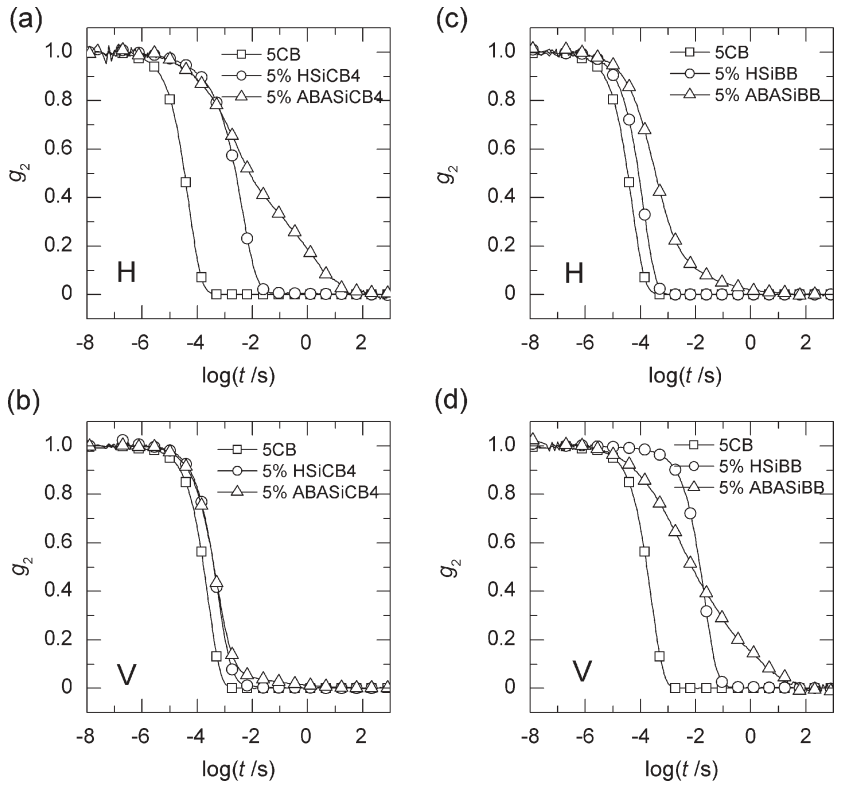


**Fig. 3** Normalized time-correlation functions, $g_2(t)$, at 25 °C and $\theta_s = 30°$ for 5CB, 5 wt% homopolymer solutions, and 5 wt% triblock copolymer gels in the H and V orientations.

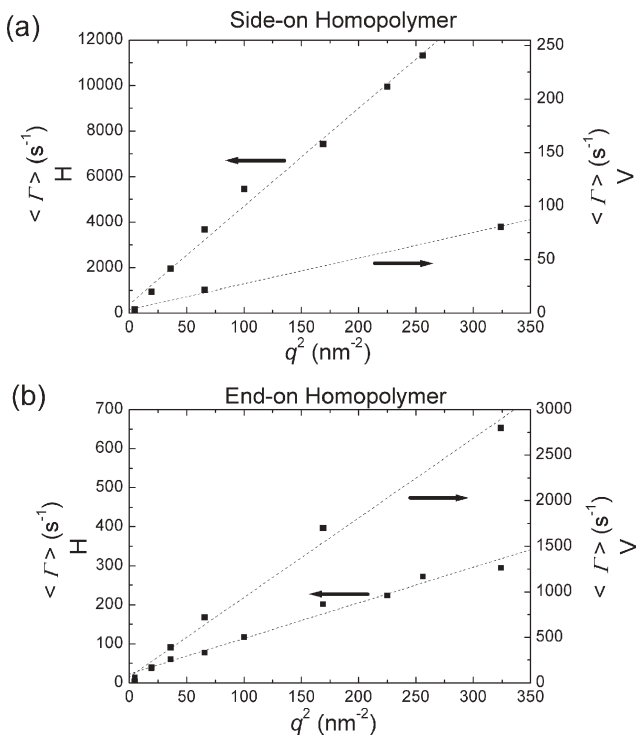


**Fig. 4** $q$-dependence of the average relaxation rates, $<\Gamma>$ for (a) 5 wt% side-on homopolymer and (b) 5 wt% end-on homopolymer in both the H and V orientations. The dashed lines are linear fits to the data points.

The triblock gels display highly broadened relaxation modes with intensity correlations extending to much longer times than for the homopolymer solution; these data could not be fitted by a conventional stretched exponential. The qualitatively different shape associated with the gel-correlation functions is apparent in both scattering geometries, but it is most dramatic in the H geometry for ABASiCB4 (Fig. 3a) and the V geometry for ABASiBB (Fig. 3d), exactly the same pairing observed for the slowing-down of director modes in the corresponding homopolymer solutions. On the other hand, in the P orientation, the slow dynamics are evident in both gels (Fig. 7).

Normalizing the delay time by $q^2 \sim [\sin(\theta_s/2)/\sin(\theta_0/2)]^2$ (where $\theta_0$ is a fixed reference angle) collapses the time-autocorrelation functions of homopolymer solutions and 5CB onto one another, demonstrating that the relaxation rate has the $q^2$-dependence associated with diffusive hydrodynamic modes (Fig. 5a, 5b, 6a, and 6b). On the other hand, the $q^2$-scaling superimposes the intensity-autocorrelation functions of end-on (ABASiCB4) triblock gels only at short times (Fig. 5c and 5d). Significant deviations are observed at long times ($>10^{-1}$ s) and lower angles ($\theta_s < 38°$). Similarly, the auto-correlation functions for both gels in the P orientation have a $\sin^2(\theta_s/2)$ scaling only at short times and deviate from this behavior at long times (Fig. 7). By contrast, in the case of side-on gels (ABASiBB), the data at 25 °C superimpose well for almost all scattering angles (Fig. 6c and 6d).

In triblock copolymer solutions of different polymer concentration, a qualitative change in the shape of the

 

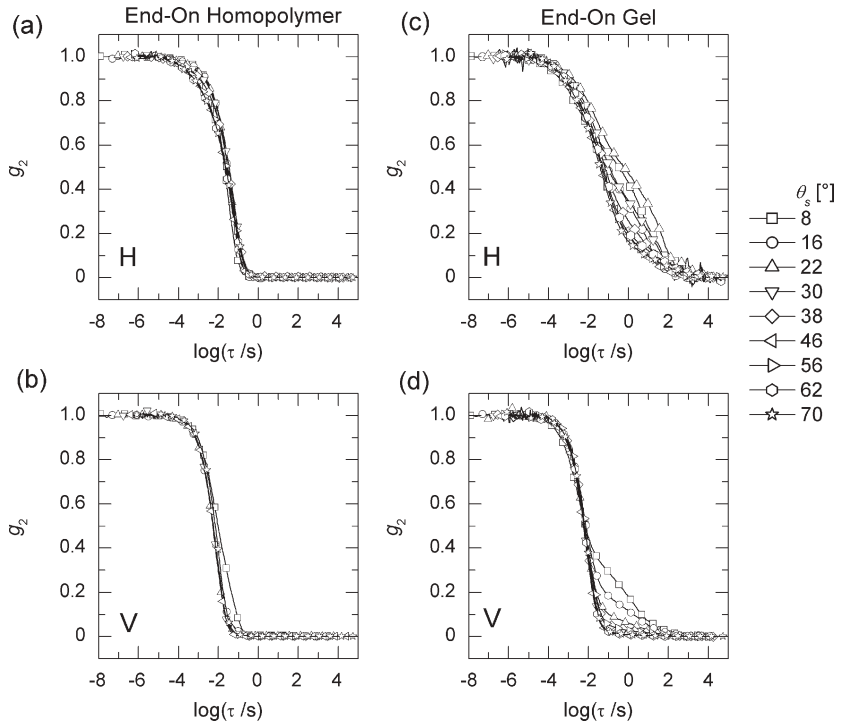


**Fig. 5** Normalized time-correlation functions, $g_2(t)$, at 25 °C of end-on polymers at a variety of scattering angles as a function of rescaled delay time, $\tau = t(\sin(\theta_s/2)/\sin(\theta_o/2))^2$, where $\theta_o = 8°$. 5 wt% end-on homopolymer (HSiCB4) in (a) H orientation and (b) V orientation; and 5 wt% end-on triblock copolymer gel (ABASiCB4) in (c) H orientation and (d) V orientation.

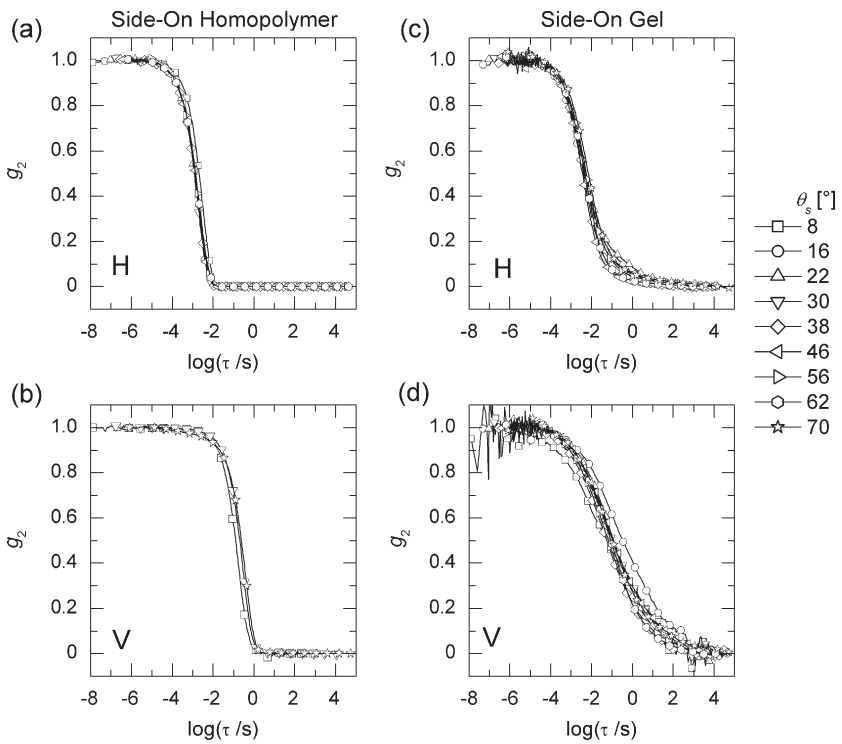


**Fig. 6** Normalized time-correlation functions, $g_2(t)$, at 25 °C of side-on polymers at a variety of scattering angles as a function of rescaled delay time, $\tau = t(\sin(\theta_s/2)/\sin(\theta_o/2))^2$, where $\theta_o = 8°$. 5 wt% Side-on homopolymer (HSiBB) in (a) H orientation and (b) V orientation; and 5 wt% side-on triblock copolymer gel (ABASiBB) in (c) H orientation and (d) V orientation.

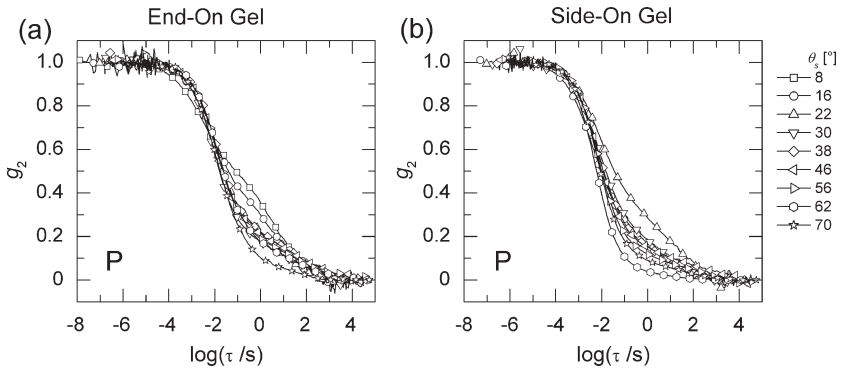


**Fig. 7** Normalized time-correlation functions, $g_2(t)$, at 25 °C of triblock copolymer solutions in P orientation at a variety of scattering angles as a function of rescaled delay time, $\tau = t(\sin(\theta_s/2)/\sin(\theta_o/2))^2$, where $\theta_o = 8°$. (a) 5 wt% End-on triblock (ABASiCB4) and (b) 5 wt% side-on triblock (ABASiBB).

intensity-autocorrelation function coincides with the gel point; the slow dynamics in the end-on (ABASiCB4) gel abruptly appear at 5 wt% concentration but are not evident at lower concentration [*e.g.*, 1 wt% (Fig. 8)]. Prior rheological studies have shown that at 5 wt% concentration end-on gels exhibit a wide plateau in their storage modulus that is characteristic of a gel.[7] Beyond the gel point, doubling and tripling the concentration has relatively mild effects (Fig. 8). The dynamics of relaxation become slower, but the shape of the correlation function is qualitatively the same.

End-on homopolymers and gels are relatively insensitive to temperature, as compared to their side-on counterparts. As temperature is increased from well-below the nematic–isotropic transition ($T_{NI}$) to within 2 °C of $T_{NI}$, the intensity-correlation functions of end-on (HSiCB4) homopolymer solution and end-on (ABASiCB4) gel hardly change (Fig. 9). In contrast, the relaxation time of side-on homopolymer in the V geometry speeds up by orders of magnitude (Fig. 10b). Changing the temperature also significantly changes the observed dynamics in side-on (ABASiBB) gels (Fig. 10c and 10d). In the H orientation, the long-time tail in the intensity-correlation function that can be seen at 25 °C almost disappears at 31.5 °C, and the initial drop-off in the decay shifts to shorter times with increasing temperature (Fig. 10c). In the V orientation, the long-time tail similarly diminishes as the temperature is increased, but the initial decay shifts to longer times (Fig. 10d). In contrast to their behavior at 25 °C (Fig. 6c and 6d), at 31.5 °C the side-on gels depart from pure $q^2$ hydrodynamic behavior at long times (Fig. 11c and 11d).

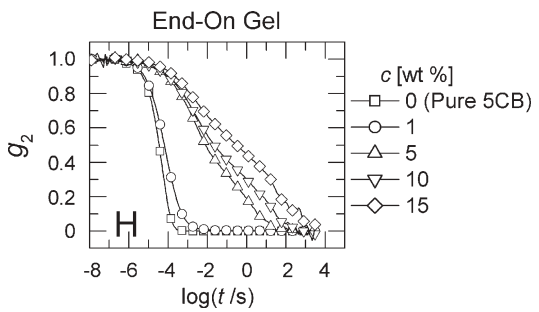


**Fig. 8** Concentration dependence of the normalized time-correlation functions, $g_2(t)$, at 25 °C and $\theta_s = 30°$ of end-on triblock copolymer gels (ABASiCB4) in the H orientation.

## Discussion

The data for the LC gels qualitatively resemble those observed from previous light-scattering studies of associating polymers,[23–29] with the appearance of slow relaxation modes above a critical concentration and highly stretched intensity-autocorrelation functions with a strong $q$-dependence. However, in the present study, the scattered light arises primarily from fluctuations in the orientation of the nematic director, not density fluctuations as in the previous light-scattering studies of gelled systems[23–29]. Therefore, structural changes such as micellar diffusion or concentration fluctuations in the polymer network are revealed indirectly by their effect on the nematic-director dynamics.

Our data indicate that in the LC physical gels at least two distinct relaxation processes couple to the director and scatter light. The faster relaxation process shows a $q^2$-scaling characteristic of hydrodynamic modes, as in homopolymer solutions and pure low molecular weight nematics. The relaxation process slows with the addition of triblock copolymer and is dependent on the polymer/gel architecture (oblate *vs.* prolate), but it remains hydrodynamic. This behavior contrasts sharply with light-scattering results on LC elastomers,[5] where the LC director modes are strictly nonhydrodynamic (relaxation rate independent of $q$), due to the full incorporation of the LC into the cross-linked polymer network and the consequent nature of the director-network coupling required by rotational invariance.[3,4,14] In contrast, our physical gels show orientational fluctuations that are soft in all directions at long wavelengths.

The slow gel dynamics expressed in the correlation data at long times are associated with long length scales; the smaller the scattering angle, the more strongly the intensity-autocorrelation persists at long time (Fig. 5c, 5d, 6c, 6d, 7a, and 7b). Indeed, the $q$-dependence of the slow relaxation appears to be stronger than $q^2$ (or $\sin^2\theta_s/2$) for small wavevectors (or low $\theta_s$), and it is reminiscent of hindered relaxational dynamics in colloidal glasses and associative polymers.[23–26,28,30] We propose that the nematic director is

 

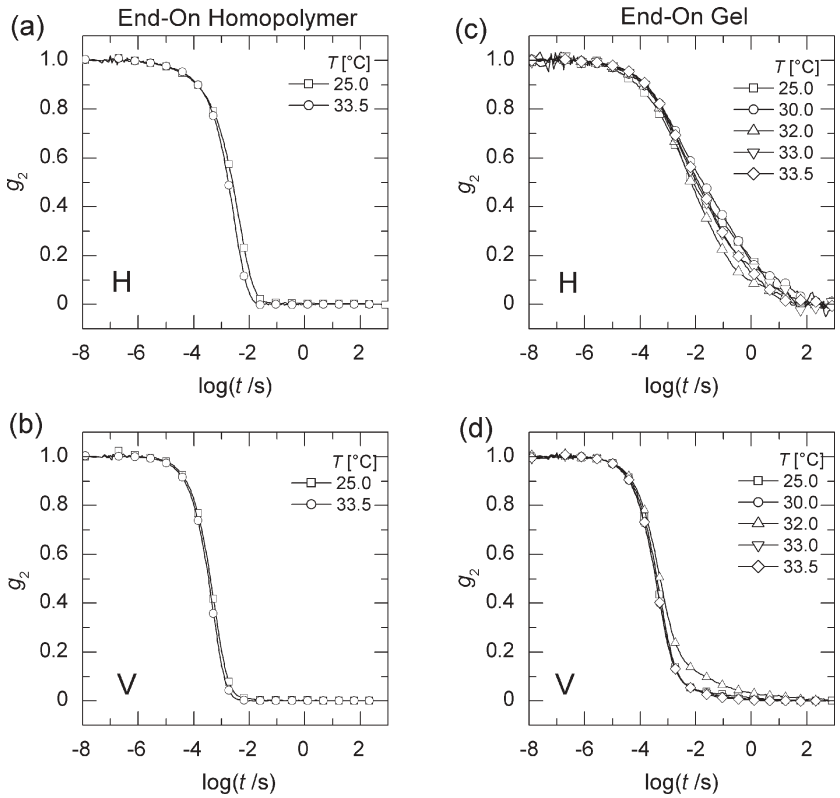


**Fig. 9** Temperature dependence of the normalized time-correlation functions, $g_2(t)$, at $\theta_s = 30^\circ$ of 5 wt% end-on homopolymer (HSiCB4) in (a) H orientation and (b) V orientation and 5 wt% end-on triblock copolymer gel (ABASiCB4) in (c) H orientation and (d) V orientation.

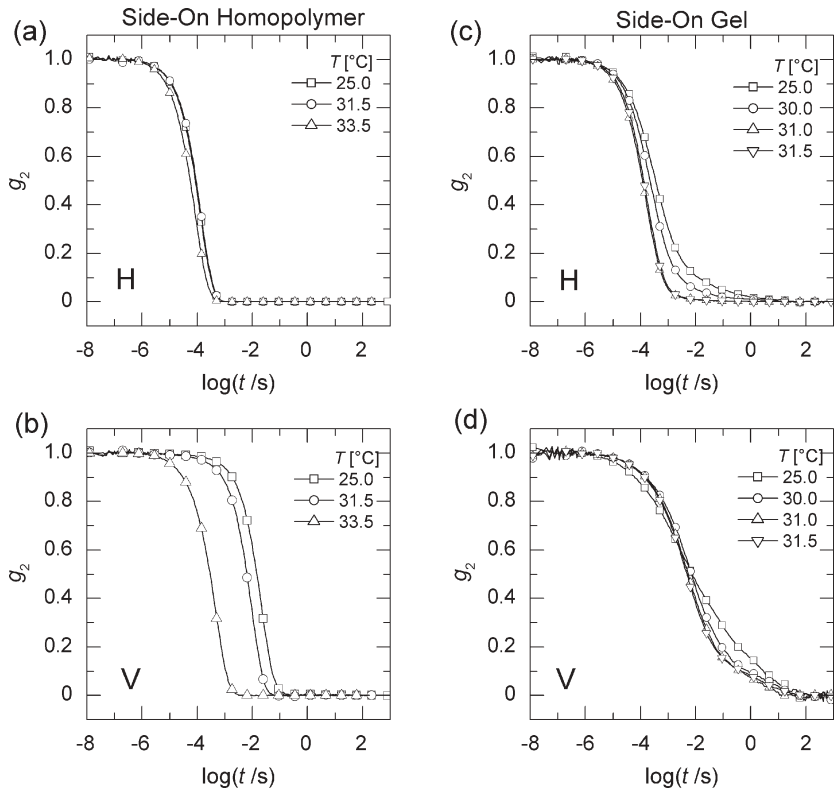


**Fig. 10** Temperature dependence of the normalized time-correlation functions, $g_2(t)$, at $\theta_s = 30^\circ$ of 5 wt% side-on homopolymer (HSiBB) in (a) H orientation and (b) V orientation and 5 wt% side-on triblock copolymer gel (ABASiBB) in (c) H orientation and (d) V orientation.

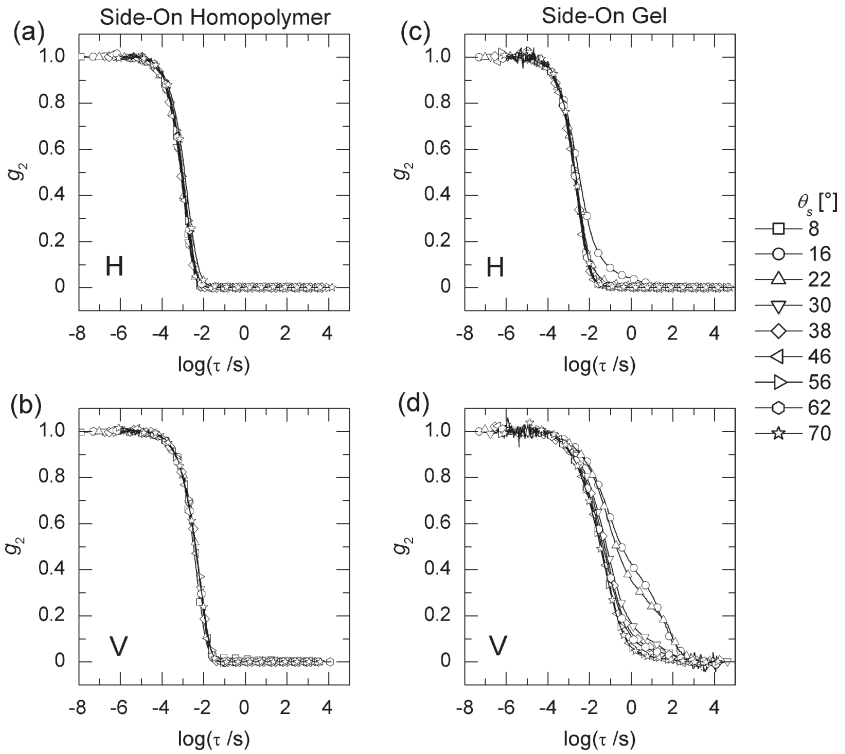


**Fig. 11** Normalized time-correlation functions, $g_2(t)$, of side-on homopolymer solution and triblock polymer gel at a variety of scattering angles as a function of rescaled delay time, $\tau = t(\sin(\theta_s/2)/\sin(\theta_o/2))^2$, where $\theta_o = 8°$. 5 wt% side-on homopolymer (ABASiBB) solution at 33.5 °C in (a) H orientation and (b) V orientation and 5 wt% side-on triblock copolymer (ABASiBB) gel at 31.5 °C in (c) H orientation and (d) V orientation.

coupled to the associated gel structure, yielding long-lived orientational fluctuations. The nematic director can relax *via* the fast relaxation mode only to a certain extent, due to a coupling to the polymer-gel structure. At long enough times, however, the physical junctions in the network reorganize and allow the nematic director to fully lose correlation with its initial orientation.

This idea is demonstrated schematically in Fig. 12. Under a deformation, the network can undergo a "fast" viscoelastic relaxation mode in which none of the physical junctions are broken. On the other hand, the physical junctions in the network are being constantly broken and reformed, and on long time scales the network can significantly reorganize its structure. This network-reorganization process can appear as a second, much slower director-relaxation mode. The picture presented in Fig. 12 is only a schematic, and in the actual gel, the polymer micelles are not ordered on a lattice.[31] However, the illustration conveys the association of polymers into micelles and the interaction of micelles by repulsive forces as well as bridging between micelles, and it qualitatively accounts for two separate relaxation modes.

Prolate (side-on) and oblate (end-on) polymer gels both strongly modify predominantly twist relaxation of the director (Fig. 7 and for lower $\theta_s$ values in Fig. 5d and 6d). However, bend and splay fluctuations are affected quite differently by the two types of gels: the end-on gel selectively in slows and stretches the relaxation of bend fluctuations (Fig. 5c) relative to splay fluctuations (Fig. 5d for larger $\theta_s$), and the side-on gel does the opposite (Fig. 6c and 6d). The viscoelastic anisotropy of the homopolymer solutions is thus reflected in the corresponding gels, pointing to an anisotropic gel structure. We envisage some combination of anisotropy in the intermicellar distance and in the connectivity of the micellar

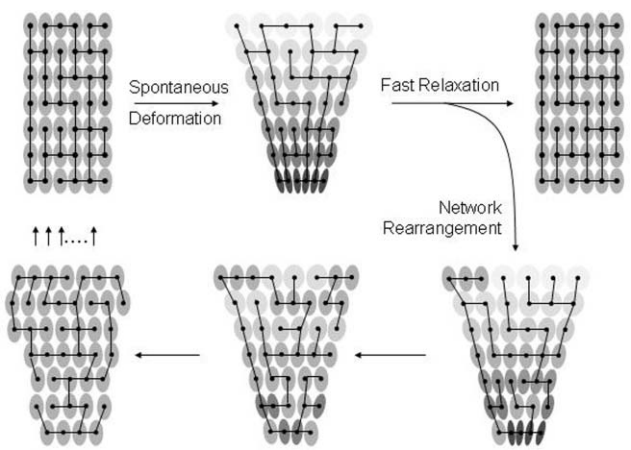


**Fig. 12** Schematic for network relaxation *via* a fast mode that retains the network structure, and a slow mode that requires the reorganization of the physical network. The ellipsoids represent polymer micelles with an SGLCP corona (grey shading), a polystyrene core (dark circle), and intermicellar bridges (dark lines). The shading represents the local density of micelle-coronal chains, with darker shading corresponding to a higher density. The schematic shows that a network deformation stretches the intermicellar bridges as well as deforming micelles. A slow network-rearrangement process re-establishes the equilibrium configuration through a combination of micelle-hopping and the nucleation or evaporation of micelles.

 

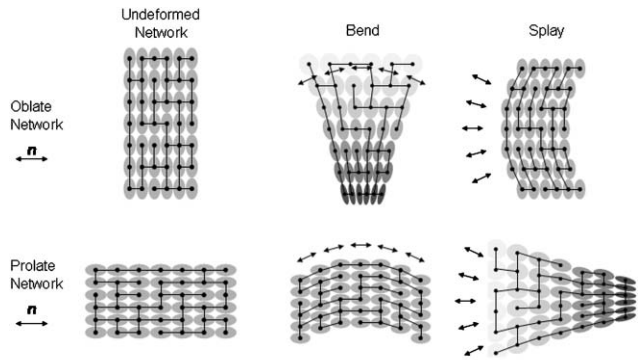


**Fig. 13** Schematic for network deformations associated with splay and bend LC deformations.

bridges, with the longer dimension of the micelles aligned along the director in a side-on gel or perpendicular to the director in an end-on gel, as depicted in Fig. 13. In this case, "undulation" (or an elastic bending) of the gel network along the long axis does not require a severe distortion of the micellar positions or stretching of the bridges: twisting or splaying of the long axis causes either a substantial reorientation of the micelles or distortion of their spacing or both. This results in a strong coupling of slow gel dynamics to twist director distortions in both gel types and a selective coupling to bend and splay director distortions, respectively, in the end-on and side-on gels (see Fig. 13).

Another aspect of anisotropic gel structure is observed in the initial decay of the correlation data – specifically, the faster initial relaxation observed in the side-on gels relative to the corresponding homopolymer solution (Fig. 3d). Interestingly, this case corresponds to the gel with the largest polymer-conformational anisotropy or aspect ratio – ($R_{//} : R_{\perp} > 5 : 1$ in the side-on compared to $R_{//} : R_{\perp} \approx 1 : 1.6$ in the end-on gel at 25 °C).[6] As temperature increases toward $T_{NI}$, the initial decay of the splay mode of the side-on gel slows (Fig. 10d), and this coincides with a decreasing network anisotropy, as confirmed by the changing relaxation rates in the side-on homopolymer solutions (Fig. 10a and 10b). Therefore, this faster initial decay is associated with more anisotropic networks. Recently, Lubensky and Stenull have predicted a modification to the elastic free energy in LC elastomers[3] that provides for an additional torque on the director that strongly depends on network anisotropy, consistent with the observation of faster director relaxation in the more anisotropic gel (the side-on gel at lower temperatures). The weaker coupling between the nematic director and network deformations in less anisotropic networks also apparently results in more widely separated relaxation dynamics and modified hydrodynamic behavior at long times (compare Fig. 5c, 5d, 11c, and 11d to Fig. 6c and 6d).

## Conclusions

Director-relaxation dynamics in LC physical gels exhibited overdamped dynamics over a broad range of time scales and with two distinct components. The faster component is hydrodynamic and corresponds to director-relaxation modes predicted by dynamic theories of homopolymer solutions, where prolate chains strongly slow splay relaxation and oblate chains strongly decreased the bend-relaxation rate. We also observed a slow component to the relaxation that increases in amplitude at low scattering angles, exhibits a stronger $q$-dependence than the faster component of the dynamics, and has a strong anisotropy that depends on the chain architecture. The slow component arises from coupling of the nematic director to the rearrangement of cross-links in the self-assembled polymer structure and is a consequence of the physical nature of the gel structure. At long enough times the gel structure reorganizes, allowing the nematic director to fully relax, resulting in the long-time decay in the observed correlation function. The network anisotropy is also manifested in the initial decay of the correlation function. The most anisotropic networks show a faster initial decay than the corresponding homopolymer solution, indicating that the network can provide an additional restoring torque on the director.

## References

1 J. T. Ho, in *Liquid Crystals*, ed. S. Kumar, Cambridge University Press, Cambridge, 2001.
2 A. M. Jamieson, D. F. Gu, F. L. Chen and S. Smith, *Prog. Polym. Sci.*, 1996, **21**, 981–1033.
3 O. Stenull and T. C. Lubensky, *Phys. Rev. E: Stat. Phys., Plasmas, Fluids, Relat. Interdiscip. Top.*, 2004, **69**, 051801.
4 E. M. Terentjev and M. Warner, *Eur. Phys. J. E*, 2001, **4**, 343–353.
5 M. Schönstein, W. Stille and G. Strobl, *Eur. Phys. J. E*, 2001, **5**, 511–517.
6 M. D. Kempe, N. R. Scruggs, R. Verduzco, J. Lal and J. A. Kornfield, *Nat. Mater.*, 2004, **3**, 177–182.
7 M. Kempe, R. Verduzco, N. R. Scruggs and J. A. Kornfield, *Soft Matter*, 2006, **2**, 422–431.
8 J. Schmidtke, S. Werner and G. Strobl, *Macromolecules*, 2000, **33**, 2922–2928.
9 D. F. Gu, A. M. Jamieson, C. Rosenblatt, D. Tomazos, M. Lee and V. Percec, *Macromolecules*, 1991, **24**, 2385–2390.
10 G. Williams and D. C. Watts, *Trans. Faraday Soc.*, 1970, **66**, 80–85.
11 G. Williams, D. C. Watts, S. B. Dev and A. M. North, *Trans. Faraday Soc.*, 1977, **67**, 1323–1335.
12 C. P. Lindsey and G. D. Patterson, *J. Chem. Phys.*, 1980, **73**, 3348–3357.
13 P. G. de Gennes, in *Liquid Crystals of One- and Two- Dimensional Order*, ed. W. Helfrich and G. Heppke, Springer, Berlin, 1980, p. 231.
14 P. D. Olmsted, *J. Phys. II*, 1994, **4**, 2215–2230.
15 P. G. de Gennes, *The Physics of Liquid Crystals*, 2nd edn., Clarendon Press, Oxford, 1993.
16 (Orsay Liquid Crystal Group) G. Durand, L. Leger, F. Rondelez and M. Veyssie, *Phys. Rev. Lett.*, 1969, **22**, 1361–1363.
17 Orsay Liquid Crystal Group, *J. Chem. Phys.*, 1969, **51**, pp. 816–822.
18 Y.-C. Chiang, A. M. Jamieson, S. Campbell, Y. Lin, N. O'Sidocky, L. C. Chien, M. Kawasumi and V. Percec, *Rheol. Acta*, 1997, **36**, 505–512.
19 Y.-C. Chiang, A. M. Jamieson, S. Campbell, T. H. Tong, N. D. Sidocky, L. C. Chien, M. Kawasumi and V. Percec, *Polymer*, 2000, **41**, 4127–4135.
20 F.-L. Chen, A. M. Jamieson, M. Kawasumi and V. Percec, *J. Polym. Sci., Part B: Polym. Phys.*, 1995, **33**, 1213–1223.
21 D. F. Gu, A. M. Jamieson, M. Kawasumi, M. Lee and V. Percec, *Macromolecules*, 1992, 25.
22 F. Brochard, *J. Polym. Sci., Part B: Polym. Phys.*, 1979, **17**, 1367–1374.
23 M. Adam, M. Delsanti and J. P. Munch, *Phys. Rev. Lett.*, 1988, **61**, 706–709.

24 V. Castelletto, I. W. Hamley and T. A. Waigh, *J. Chem. Phys.*, 2004, **121**, 11474–11480.
25 C. Konák, G. Fleischer, Z. Tuzar and R. Bansil, *J. Polym. Sci., Part B: Polym. Phys.*, 2000, **38**, 1312–1322.
26 C. Konák, M. Helmstedt and R. Bansil, *Macromolecules*, 1997, **30**, 4342–4346.
27 J. Martin and J. Wilcoxon, *Phys. Rev. Lett.*, 1988, **61**, 373–376.
28 E. Raspaúd, D. Lairez, M. Adam and J.-P. Carton, *Macromolecules*, 1996, **29**, 1269–1277.
29 B. Nyström and B. Lindman, *Macromolecules*, 1995, **28**, 967–974.
30 J. E. Martin, J. Wilcoxon and J. Odinek, *Phys. Rev. A: At., Mol., Opt. Phys.*, 1991, **43**, 858–872.
31 N. R. Scruggs, J. A. Kornfield and J. Lal, *Macromolecules*, 2006, **39**, 3921–3926.



 